Covalent Binding of a Carcinogen as a Probe for the Dynamics of Deoxyribonucleic Acid†

M. P. Daune,*,‡ E. Westhof,§ N. Koffel-Schwartz,‡ and R. P. P. Fuchs‡

Laboratoire de Biophysique et Laboratoire de Cristallographie Biologique, Institut de Biologie Moléculaire et Cellulaire du C.N.R.S., 67084 Strasbourg Cedex, France

Received July 13, 1984

ABSTRACT: In order to determine the kinetic parameters of the binding to DNA of two closely related ultimate carcinogens, 2-(*N*-acetoxy-*N*-acetylamino)fluorene (N-Aco-AAF) and 2-(*N*-hydroxyamino)fluorene (N-OH-AF), three kinds of experiments were performed: measurement of the final amount of adduct (N-Aco-AAF and N-OH-AF), determination of the initial rate, and study of the reaction with deoxyguanosine (N-Aco-AAF only) at temperatures between 4 and 50 °C. The kinetic treatment of the chemical equations relies on two main assumptions: (i) binding of carcinogen to the C_8 of guanine (G) could occur either with the classical B conformation or with a transient conformational state of the sugar–phosphate chain at the level of the guanine and denoted by G*; (ii) the equilibrium between G and G* is fast as compared to the chemical rate of carcinogen binding. These two assumptions have been verified by comparing experimental and calculated values of some of the data. From experimental data it is possible then to determine the characteristic independent parameters of the reaction: the constant K of the G $\rightleftarrows$ G* equilibrium and the enthalpy change ΔH of the process, the rate constant k_3 of the binding to the C_8 of G, and the rate constant k_1 of hydrolysis of the carcinogen with their corresponding activation enthalpies E^*_3 and E^*_1. Some essential results obtained are as follows: (a) The amount of G* that represents about 10% of the G at room temperature increases with temperature and is higher in denatured than in native DNA. (b) The values of ΔH ($\sim$9 kcal mol^{-1}) and ΔS ($\sim$27 cal K^{-1} mol^{-1}) of the G $\rightleftarrows$ G* equilibrium are close to those associated with single base pair opening [Wartell, R. M., & Benight, A. S. (1982) *Biopolymers 21*, 2069]. (c) N-Aco-AAF reacts only with the G* conformation while N-OH-AF binds preferentially to the "classical" G (B conformation). Therefore, the electrophilic carcinogens behave as probes of the dynamic state of the DNA, but the rate of the G $\rightleftarrows$ G* exchange is fast as compared to the binding rate of the carcinogen. To relate these observations to the structure of DNA, a model is proposed according to which the G $\rightleftarrows$ G* equilibrium corresponds to a conformational change of the phosphodiester backbone bringing the torsion angle C(3′)–C(4′)–C(5′)–O(5′) from gauche$^+$ to trans and the torsion angle C(5′)–O(5′)–P–O(3′) from gauche$^-$ to trans conformation. Such a "crankshaft" motion, which could be triggered by pseudorotational fluctuations of the sugar, considerably increases the O(5′)···C_8 distance between the phosphate group and the guanine, without modifying significantly the distance between two adjacent phosphate groups. Following the covalent binding, a structural rearrangement occurs that can depend on the chemical properties of the carcinogen and on the DNA base sequence. The use of this model in premelting phenoma, proton exchange, and B → Z transition is discussed.

More than 10 years ago, a dynamic aspect of the DNA double helix was suggested in order to explain the covalent binding of the hepato carcinogen 2-(*N*-acetoxy-*N*-acetylamino)fluorene (N-Aco-AAF)[1] to the poorly accessible C_8 of the guanine residue (Kapuler & Michelson, 1971). Following the hypothesis of Printz & Von Hippel (1968) that exchange of interchain hydrogens occurs in a local, transiently open conformational state, brought about by thermally induced local fluctuations ("breathing" modes), a local conformational change of the double helix, allowing the C_8 atom to be accessible during a short period of time, could be conceived. During these last 10 years many experimental data have provided evidence for an internal dynamics of the DNA molecule: tritium or deuterium exchanges (McConnell & Von Hippel, 1970; Teitelbaum & Englander, 1975; Mandal et al., 1979; Woodward & Hilton, 1979), premelting behavior (Palecek, 1976), time-resolved fluorescence of intercalated dyes (Wahl et al., 1970; Genest & Wahl, 1978), ESR of spin-labeled intercalating dyes (Hurley et al., 1982), kinetics of intercalation (Ramstein & Leng, 1975; Bresloff & Crothers, 1975; Strum et al., 1975), NMR (Hogan & Jardetzky, 1979; Early & Kearns, 1979; Bolton & James, 1980), Raman (Urabe & Tominaga, 1982), or microwave (Van Zandt et al., 1982; Swicord & Davis, 1982) spectroscopies, and dynamic light scattering (Wilcoxon & Schurr, 1983). From some of these studies (NMR, ESR, fluorescence, and dynamic light scattering), DNA flexibility can be understood as rapid motions of the sugar–phosphate backbone between torsional minima on a nanosecond time scale. However, from deuterium exchange studies, time constants for base-pair opening of the order of 1 s^{-1} were found, while relaxation times of intercalated planar aromatic dyes are between 18 and 40 μs.

At the same time, several static or dynamic models of local distortion of the helix were proposed on the basis of either structural features like "kinks" (Crick & Klug, 1975; Sobell

† This work was supported by grants from the L.N.F.C.C. (Comité du Haut-Rhin), the C.N.R.S. (ASP 6383), and the F.N.C.L.C.C.

‡ Laboratoire de Biophysique, Institut de Biologie Moléculaire et Cellulaire du C.N.R.S.

§ Laboratoire de Cristallographie Biologique, Institut de Biologie Moléculaire et Cellulaire du C.N.R.S.

[1] Abbreviations: N-Aco-AAF, 2-(*N*-acetoxy-*N*-acetylamino)fluorene; AAF, 2-(*N*-acetylamino)fluorene residue bound to guanine; N-OH-AF, 2-(*N*-hydroxyamino)fluorene; AF, 2-aminofluorene residue bound to guanine; dGuo, deoxyguanosine; nDNA and dDNA, native DNA and denatured DNA; T_m, melting temperature of DNA.

0006-2960/85/0424-2275$01.50/0

et al., 1977) or mechanical properties like propagation of a torsional wave (Simon, 1971; Barkley & Zimm, 1979) or of a soliton wave (Englander et al., 1980).

The mechanical parameters used in the latter models have in general no precise relationship with the structural parameters used in the former ones. With the extension of the concept of pseudorotation (Kilpatrick et al., 1947) to the furanose ring (Altona & Sundaralingam, 1972), the sugar can be viewed as a continuum of puckered states accessible through small but correlated changes of the ring torsion angles. Beside the preferred C(2′)-endo and C(3′)-endo puckers, a series of intermediate conformations exist in a transient state. In those transient conformations, the short-range interactions, which stabilize the preferred states, are weakened and other combinations of conformations can occur. Thus, thermal fluctuations will continuously excite the pseudorotational states of the sugar ring leading to changes in the relative orientations of the base and of the phosphate and to twisting and bending fluctuations (Sundaralingam & Westhof, 1981). Because of correlations between the torsion angles of the sugar–phosphate backbone, most of the torsional fluctuations do not lead to large reorientations of the bases (Sundaralingam & Westhof, 1980; Olson, 1981; Keepers et al., 1982; Kollman et al., 1982). In this way, the "rigid" view of DNA gained from hydrodynamic studies can be reconciled with the "flexible" view of DNA revealed by several spectroscopies. However, while torsional oscillations are expected to be rapid and on the nanosecond time scale, the fluctuational base-pair opening in native polynucleotide duplexes has a half-life around 1 s (Mandal et al., 1979; Preisler et al., 1981). This is reflected in the activation energies (15–20 kcal/mol) for the rates in both directions (Early et al., 1981; Preisler et al., 1981). It is known also that exchange occurs via a single base pair opening mechanism without opening of neighboring base pairs. Also, the thermodynamics parameters indicate that H exchange is a premelting phenomenon that does not reflect the same process as the helix–coil melting transition (Mirau & Kearns, 1983; Preisler et al., 1981). The occurrence of correlated crankshaft motions in the sugar–phosphate backbone (Sundaralingam & Westhof, 1981; Olson, 1981) could explain those observations, since they can occur in a hydrogen-bonded duplex structure without leading to more than a local alteration in a single base pair.

In this paper, the local dynamics of the sugar coupled to crankshaft motions in the sugar–phosphate backbone was considered as the primary event triggering conformational changes in the polynucleotide backbone and leading, among others, to the movement that allows the C_8 to become accessible to the bulky electrophilic reagent. Such an interpretation was already proposed as a tentative model (Daune, 1983; Westhof, 1983).

In order to obtain information about those dynamic states, we have studied the binding kinetics to native and denatured DNA of two closely related ultimate carcinogens, N-Aco-AAF and 2-(*N*-hydroxyamino)fluorene (N-OH-AAF). These two carcinogens were chosen because, although they both react with the C_8 of guanine residues, they behave very differently in their reactions with nucleic acids. Thus, while N-Aco-AAF reacts better with denatured than with native DNA (Kapuler & Michelson, 1971), the opposite is true for N-OH-AF (Spodheim-Maurizot et al., 1979). Also, N-Aco-AAF binds equally well to both the B and the Z forms of poly[d(G-C)] but N-OH-AF binds only the B form (Rio & Leng, 1983). And finally, the B to Z transition is facilitated in AAF-modified poly[d(G-C)] (Sage & Leng, 1980; Santella et al., 1981a), which is not the case with AF-modified poly[d(G-C)] (Sage & Leng, 1980). From those studies, it can be inferred that these two carcinogens react with guanine residues in different conformational states in the DNA double helix and, conceivably, could act as probes of the DNA dynamics governing the conformational transitions.

Carcinogen binding was followed in different ways and in a reasonable range of temperatures (4–50 °C). From the whole set of experimental data, the kinetic and thermodynamic parameters that characterize both the chemical reactions and the DNA conformational equilibrium have been determined. The working hypothesis used in their calculations could be further verified. According to these results, a new model of local dynamics at the level of a guanine residue is proposed, which is able not only to explain the observed process but also to offer an explanation for other phenomena related to the dynamics of the DNA molecule.

Materials and Methods

Binding of N-Aco-AAF and N-OH-AF to DNA. Calf thymus DNA was used in all the experiments. Heat-denatured DNA was obtained after heating native DNA for 10 min at 100 °C followed by rapid cooling in ice. Reaction with N-Aco-AAF (^{3}H ring sp act. 167 mCi/mmol) or N-OH-AF (^{3}H ring sp act. 62 mCi/mmol) was performed in 20% ethanol containing sodium citrate buffer, 2×10^{-3} M (or 10^{-2} M), at pH 7.0 and pH 5.5, respectively. In the case of N-Aco-AAF the reaction was stopped by four successive ethanol precipitation–redissolution cycles. With N-OH-AF the solvolysis products were extracted by a mixture of phenol–Sevag (1:1) followed by a Sevag extraction, and the modified DNA was recovered from two ethanol precipitation–redissolution cycles. The extent of modification, i.e., the amount of modified base pairs, was determined as described previously (de Murcia et al., 1979). For each temperature the final amount of DNA modification was determined by allowing the reaction to proceed for a period of time at least equal to 3 times the value of the half-life of the solvolysis reaction of the reagent at 4 °C (~20 h).

Binding of N-Aco-AAF to Deoxyguanosine (dGuo). In order to follow the adduct concentration with time (the rate of dGuo–AAF formation), we have taken advantage of an absorbance change of the medium. By using the classical four-cells method (N-Aco-AAF in cell I, dGuo in cell II, reaction mixture in cell III, and pure solvent, i.e., 2×10^{-3} M citrate buffer with 20% ethanol at pH 7, in cell IV), the evolution with time of the difference of absorbance at 275 nm was directly recorded on a Cary 118 C spectrophotometer with the full-scale sensitivity of 0.02 absorbance unit. Special care was taken in delivering the solution in each of the four cells (5-mm optical path) to maintain an accurate balance of concentration since the total absorbance along each optical path was close to 1.

Kinetic Equations and Experimental Results

Covalent binding of the carcinogen to the C_8 of guanine was proved to be a nucleophilic substitution (Miller, 1970) with the strong electrophilic nitrenium ion leading to a C–N bond between guanine and fluorene aromatic ring (arylamidation). We have however to assume that in mose cases the C_8 of G is only accessible to the reagent when the nucleotide conformation of the guanine residue differs from the classical B structure. This new transient structure will be denoted G*. The electrophilic reagent can also react with water, and this hydrolysis, leading to an inactive compound C_1, has to be taken into account as a competition reaction. In fact, several deg-

radation products are issued from the hydrolysis reaction (De Baun et al., 1970), and eq 1 can be viewed as a coarse approximation but sufficient for our purpose. In view of the high concentration of water (55 M) compared to that of reagent (10^{-4} M), this hydrolysis can be treated as a pseudo-first-order reaction.

The whole process can thus be described by the three following reactions (where C designates the carcinogen and A the adduct):

hydrolysis

$$C \xrightarrow{k_1} C_1 \tag{1}$$

conformational change

$$G \underset{k_{-2}}{\overset{k_2}{\rightleftharpoons}} G^* \tag{2}$$

irreversible binding to give an adduct A with either G or G*

$$G^* + C \xrightarrow{k_3} A \tag{3}$$

$$G + C \xrightarrow{k_3} A \tag{4}$$

Note that k_1, k_2, and k_{-2} are expressed in s^{-1}, but k_3 is in L mol^{-1} s^{-1}.

In reaction 2 $K = k_2/k_{-2}$ will denote the equilibrium constant. Reaction 3 is representative of any ultimate carcinogen for which the binding can only occur with the transient G* structure. Reaction 4 on the other hand is taking place with the C_8 of guanine is readily accessible as obviously in the case of the deoxyguanosine. However and for sterical reasons, a class of ultimate carcinogens can bind to a classical G residue, and N-OH-AF will be found to illustrate this kind of carcinogen. Kinetic equations are obtained in each case by combining either eq 1, 2, and 3 or eq 1, 2, and 4. From these sets of equations it is thus possible to obtain relationships between observable quantities and characteristic parameters of the reactions.

Three types of experiments were made in order to determine the different kinetic parameters: measurement of the final amount of adduct, determination of the initial rate, and determination of the reaction rate of dGuo with the carcinogen. A kinetic treatment was made specifically for each case, leading to characteristic plots for each of the three sets of experiments.

Measurement of Final Amount of Adduct. This first approach can be considered as the classical manner of measuring the binding of a carcinogen. At zero time, $a = C_0/G_0$ is the ratio between the initial concentration of carcinogen and that of guanine (generally $a = 0.476$). At the end of the process $R = A/G_0$ is the experimentally determined ratio between the adduct A present in the DNA molecule and the amount G_0 of potential binding sites. At any time, concentrations of reagent and product must satisfy two relations:

$$C_0 = C + C_1 + A \tag{5}$$

$$G_0 = G + G^* + A \tag{6}$$

where now capital letters designate the concentrations. Let us introduct the following dimensionless parameters:

$$X_1 = C_1/C_0 \qquad X_2 = A/C_0 \tag{7}$$

(a) At first we will assume the binding as occurring only with G*, then the two following kinetic equations are readily obtained:

$$dX_1/dt = k_1(1 - X_1 - X_2) \tag{8}$$

$$dX_2/dt = k_3G^*(1 - X_1 - X_2) \tag{9}$$

Table I: Final Amount of AAF Binding to DNA at Different Temperatures As Expressed in Percentage of Modified Bases

buffer		t (°C) 4	10	20	37	50
2×10^{-3} M citrate, pH 7	nDNA	0.97	nd	1.58	2.01	3.66
	dDNA	2.95	nd	4.50	4.58	3.50
10^{-2} M citrate, pH 7	nDNA	0.13	0.19	0.25	0.32	0.48
	dDNA	0.60	0.77	1.20	1.00	nd

In order to relate G* to G, the conformational change is assumed to be fast enough to offer at any time a small concentration of G* given by

$$G^* = KG \tag{10}$$

where K is the equilibrium constant of the transconformation ($K \ll 1$). In other words, it is assumed that the chemical reaction between G* and the electrophilic reagent is always much slower than the G $\rightleftarrows$ G* conformational change.

From (10) and (6), one gets

$$G^* = \frac{K}{1 + K}G_0(1 - aX_2) \tag{11}$$

By combining (11), (8), and (9) and rearranging one obtains

$$\frac{dX_2}{1 - aX_2} = m dX_1 \tag{12}$$

where

$$m = \frac{k_3}{k_1}G_0\frac{K}{1 + K} \tag{13}$$

With the initial conditions $X_1 = X_2 = 0$, eq 12 leads to

$$\ln (1 - aX_2) = -amX_1 \tag{14}$$

This relationship between X_1 and X_2 is still valid at the end of the reaction. If $X_{1,L}$ and $X_{2,L}$ are the limiting values of the two parameters, respectively, they satisfy obviously

$$X_{1,L} = 1 - X_{2,L} \tag{15}$$

If $R = aX_{2,L}$ and using (15), one finally obtains

$$\ln (1 - R) = m(R - a) \tag{16}$$

and then from (16)

$$m = \frac{\ln (1 - R)}{R - a} \tag{17}$$

The case is illustrated with the binding of 2-(*N*-acetoxy-*N*-acetylamino)fluorene (N-Aco-AAF) to DNA. The final absorbance at 260 nm was 10. The initial carcinogen/nucleotide ratio was 0.1, corresponding to a C_0/G_0 value of 0.476.

In Table I are given the data corresponding to the two sets of experiments made with N-Aco-AAF and both native and denatured DNA in 2×10^{-3} and 10^{-2} M citrate buffer, respectively. The final amount of adduct is expressed usually as the percentage of modified bases, from which values of m can be determined according to eq 17. According to (13), the derivative of ln m with $1/T$ is equal to

$$\frac{d \ln m}{d(1/T)} = -\frac{E^*_3}{R} + \frac{E^*_1}{R} - \frac{\Delta H}{(1 + K)R} \tag{18}$$

where E^*_3 and E^*_1 are the activation energies of the chemical binding and the solvolysis of the carcinogen, respectively, and ΔH is the enthalpy change accompanying the G $\rightleftarrows$ G* transconformation. Plots of ln m vs. $1/T$ are only linear in the case of native DNA, which corresponds to the fact that K is small compared to 1 in eq 18 and cannot introduce any detectable curvature. This is no more true in the case of denatured DNA, and therefore, a straight line cannot be drawn

Table II: Final Amount of AF Binding to DNA at Different Temperatures (in 10^{-2} M Citrate Buffer, pH 5.5) As Expressed in Percentage of Modified Bases

	t (°C)					
	4	10	15	20	37	50
nDNA	0.99	1.41	2.30	3.43	4.81	3.29
dDNA	0.98	1.51	2.06	2.18	2.18	nd

through the experimental points. However, as shown later (see Interpretation of the Results) a comparison can be made between experimental values of m and calculated ones from other experiments.

In 2×10^{-3} M citrate buffer, the value of 50 °C for native DNA is almost the same as that determined at the same temperature for denatured DNA. The slopes are equal to 6.2 and 5.0 kcal/mol in 2×10^{-3} and in 10^{-2} M, respectively. This slight difference between the slopes is not significant, and a common value of about 5–6 kcal/mol could be adopted for both cases, which represent, according to (18), the balance between the three quantities $E^{\ddagger}_3$, $E^{\ddagger}_1$, and ΔH.

(b) On the other hand, when carcinogen binding is assumed to occur only with G ("classical" conformation), a parallel kinetic treatment can be developed. Instead of (17) one obtained finally

$$\frac{m}{K} = \frac{\ln (1 - R)}{R - a} \tag{19}$$

with

$$\frac{m}{K} = \frac{k_3}{k_1} \frac{G_0}{1 + K} \tag{20}$$

Because K is generally smaller than 1, variations of K in a small range of temperature can be considered as negligible compared to 1. From the dependence of m/K given by (20) with $1/T$ one can thus calculate the difference between the two activation energies corresponding to arylamidation and hydrolysis, respectively.

We assume for the moment that such a reaction scheme is valid in the case of 2-(*N*-hydroxyamino)fluorene (N-OH-AF). We give in Table II the data corresponding to the experiments made with N-OH-AF and both native and denatured DNA in 10^{-2} M citrate buffer, pH 5.5. According to eq 19 the parameter m has to be replaced by m/K. The expression of m/K (see eq 19) is now

$$\frac{m}{K} = \frac{k_3'}{k_1'} G_0 \frac{1}{1 + K}$$

where the k_3 and k_1 values relative to N-Aco-AAF have to be replaced by k_3' and k_1' relative to N-OH-AF. Between 4 and 15 °C, the values for dDNA are almost identical with those obtained with nDNA and lie on a straight line with a slope of 12 kcal/mol. The low value obtained at 50 °C is unexplained, since in this ionic strength the melting temperature is around 70 °C.

Determination of Initial Rate. The conformational change from G to G* can be viewed as the passage from a "closed" to an "open" structure so that we could use the terminology and the treatment developed in this case (Printz & Von Hippel, 1968; McConnell & Von Hippel, 1970) in which an open $\rightleftarrows$ close process is coupled with a chemical process (formaldehyde binding or isotope exchange). In order to take into account only the two reactions 2 and 3, the following conditions must be fulfilled: (a) carcinogen binding must be of the first type, i.e., reacting preferentially with G*; (b) G* as well as free deoxyguanosine leads to the same type of chemical reaction (nucleophilic substitution) with the carcinogen, and the rate constant is the same in the two cases; (c) there must be negligible hydrolysis; i.e., the binding process has to be examined in the first minutes following the initial mixture and in such conditions of concentration as to consider C as a constant C_0; (d) the concentration of carcinogen is in large excess as compared to that of nucleotides, and the binding to G can be viewed as a pseudo-first-order process.

Table III: Least-Squares Values of k_{obsd} and k_3 (L mol^{-1} s^{-1}) (See Figure 6)[a]

	t (°C)				
	4	8	20	37	50
dX_2/dt (s^{-1}) = k_3G^*	3.12×10^{-7}		3.75×10^{-6}	1.9×10^{-5}	nd
k_{obsd} = k_3G^*/G_0	4.9×10^{-3}		5.9×10^{-2}	0.3	
dX_2/dt = k_3G^*	1.83×10^{-6}		1.39×10^{-5}	8.42×10^{-5}	nd
k^d_{obsd} = k_3G^*/G_0	2.88×10^{-2}		0.217	1.32	
k_3		0.177	0.524	1.5	4.27

[a] The first two rows correspond to native DNA and the next two ones to denatured DNA. k_3 values determined from binding kinetic experiments with dGuo are given in the last row.

For experimental reasons (carcinogen solubility) this last assumption is never met and we have to rely on the classical kinetic equation (9) which gives the rate of adduct formation. The initial slope, as determined experimentally, is thus equal to k_3G^*. Recall that k_3 (in L mol^{-1} s^{-1}) denotes the rate constant of carcinogen binding to G*. In order to make a better comparison with the rate constant k_3 of carcinogen binding to deoxyguanosine, we will define k_{obsd} (in L mol^{-1} s^{-1}) by $k_{obsd} = k_3G^*/G_0$. Initial rates were determined experimentally only in the case of N-Aco-AAF in 2×10^{-3} M sodium citrate buffer. Initial absorbance at 260 nm was 1 ($G_0 = 0.636$ 10^{-4} M).

The experimental kinetic curves of adduct formation in the case of nDNA and dDNA are straight lines. From their slopes one can calculate k_{obsd}, the values of which are given in Table III. When ln k_{obsd} is plotted vs. $1/T$, two almost parallel straight lines are obtained with native and denatured DNA giving a slope of 20 and 21.4 kcal/mol for native and denatured DNA, respectively.

Reaction Rate of Deoxyguanosine (dGuo). As stated above, the reaction occurs with the classical conformation of dGuo since, in absence of the phosphate group, sterical factors in the approach of the ultimate carcinogen no longer play a role. In this case, the binding and the competitive hydrolysis are described by eq 1 and 4. With the same parameters X_1 and X_2, one gets readily

$$dX_2/dt = k_3G_0(1 - aX_2)(1 - X_1 - X_2) \tag{21}$$

When plotting X_2 vs. time, the initial slope is the limiting value of dX_2/dt when X_1 and X_2 tend to zero:

$$(dX_2/dt)_{initial} = k_3G_0 \tag{22}$$

With dGuo, k_3 was supposed to be a constant for a given carcinogen and only characteristic of the rate of binding to the C_8 of guanine residue, whatever its conformational state relative to the sugar. Experiments were conducted at 8, 20, 37, and 50 °C with a dGuo concentration of 3.3×10^{-5} M and a carcinogen/nucleotide ratio of 1. The solution of carcinogen was preheated at each of the different temperatures before adding it to the dGuo solution.

Spectrophotometric tracings of the kinetics as followed by absorbance at 275 nm are given in Figure 1. The signal to

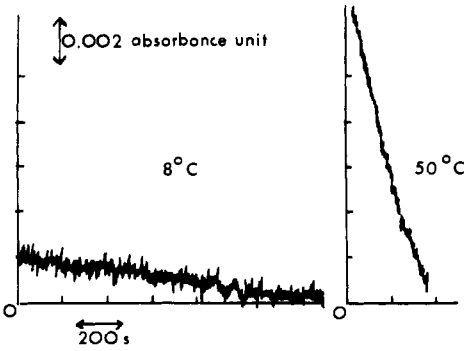

FIGURE 1: Spectrophotometric tracings of the kinetics of the reaction of deoxyguanosine with N-Aco-AAF. The absorbance at 275 nm is followed with time.

Table IV: Values of Equilibrium Constant K of the G $\rightleftarrows$ G* Transconformation for Native and Denatured DNA at Different Temperatures with the Resulting Percentage Concentration of G*

	t (°C)				
	4	8	20	37	50
G^*/G_0	(0.04)	(0.056)	0.113	0.2	(0.3)
$K_N \times 10^2$	4.17	6.0	12.7	25.0	43
G^*/G_0	(0.236)	(0.265)	0.44	0.88	
$K_D \times 10^2$	30	36	72	730	

noise ratio was high enough to determine the initial slope with a good accuracy. Corresponding values of k_3 are given in Table III. When ln k_3 is plotted vs. $1/T$, a straight line is obtained leading to a value of the activation energy $E^{\ddagger}_3$ equal to 13.1 kcal/mol.

Interpretation of the Results

In the process of carcinogen binding to DNA, six independent parameters are necessary to describe the system: K, the equilibrium constant between G and G*; k_3, the rate constant of binding to the C_8 of guanine; k_1, an average rate constant of hydrolysis and the corresponding thermodynamic quantities; ΔH, the enthalpy of the conformational change; $E^{\ddagger}_3$ and $E^{\ddagger}_1$, the activation enthalpies of reactions 3 and 1, respectively. From our data each of these parameters can be determined and the process completely described at least in the case of N-Aco-AAF.

(a) Both the rate constant k_3 and the activation enthalpy $E^{\ddagger}_3$ = 13.1 kcal/mol are readily obtained from binding studies on deoxyguanosine.

(b) From the values of $k_{obsd} = k_3 G^*/G_0$, the ratio $y = G^*/G_0$ and the value of $K = y/(1 - y)$ can be calculated. K values corresponding to native and denatured DNA are given in Table IV. Temperatures at which k_3 and k_{obsd} were measured are not always the same, and the values of G^*/G_0 that are into brackets correspond to extrapolated or interpolated values of k_3 or k_{obsd} obtained by least-squares fitting of the data.

Apparently, the ratio G^*/G_0 is unexpectedly high since at 20 °C more than 10% of the guanines in average can be found in the G* conformation, but it should be remembered that the process monitored is limited to guanine residues and that nothing can be said on the configurational changes of other bases. The fact of getting values of G^*/G_0 close to 1, at 37 °C in denatured DNA is not surprising. However, the ratios G^*/G_0 we have obtained are upper limits. Indeed, k_{obsd} is maximum when the concentration of carcinogen is taken equal to that of the bulk. If the local concentration of carcinogen around the DNA is higher (because of the hydrophobicity of the "inside" DNA), the resulting k_{obsd} would be smaller and accordingly the value of G^*. Also, the value of k_3 we used is that of dGuo reacting with AAF. If the value of k_3 for G* reacting with AAF is higher (because of favorable electrostatic interactions, for example), the resulting G^*/G_0 ratio would be also smaller.

Table V: Comparison between Experimental Values (See Eq 17) and Values of the Parameter m of Denatured DNA Calculated (See Eq 13 and 23) with the Values of K_N and K_D Previously Determined (See Table IV), First in 2×10^{-3} and Then in 10^{-2} M Citrate Buffer

		t (°C)			
		4	20	37	50
	w (eq 26)	(5.76)	3.7	4.4	
2×10^{-3} M	m_N	0.11	0.19	0.26	
citrate buffer	m_D (calcd)	(0.63)	0.72	1.16	
	m_D (exptl)	0.45	0.92	0.95	
10^{-2} M	m_N	0.013	0.026	0.033	
citrate buffer	m_D (calcd)	(0.076)	0.096	0.145	
	m_D (exptl)	0.063	0.140	0.114	
	$k_1 \times 10^5$ (s^{-1})	0.29	2	7.6	13.38

The thermodynamic parameters that characterize the G $\rightleftarrows$ G* transconformation can be determined by plotting log K vs. $1/T$. In the case of native DNA, the slope corresponds to a ΔH_0 value of 9.2 kcal/mol. With denatured DNA, the same slope is found in the range 4–20 °C. Using the K values at 20 °C, the entropy changes ΔS_0 can be calculated and are found to be 27 and 32 cal K^{-1} (base pair)$^{-1}$ for native and denatured DNA, respectively. Thus, the higher value of K_d as compared to K_n can be explained in terms of an entropy effect.

(c) From the definition of m (13) and the values of k_3 and G^* previously obtained, k_1 can be estimated in the case of N-Aco-AAF from the relation

$$k_1 = G_0 k_{obsd}/m$$

in which $G_0 = 0.636 \times 10^{-4}$ M. The values of k_1 can be found at the bottom of Table V. From the slope of the linear plot of ln k_1 with $1/T$, an activation energy of about 15.0 kcal/mol can be estimated. The rate of solvolysis obtained at 50 °C ($\sim 0.13 \times 10^{-3}$ s^{-1}) is smaller than that given by Fuchs et al. (1981) at 45 °C (0.32×10^{-3} s^{-1}), but in view of the poor accuracy of our present indirect estimation, the discrepancy is not too serious. A complete set of the six parameters is thus obtained in the case of N-Aco-AAF. In this interpretation of the results, m values are obtained under the assumption of a fast exchange between G* and G, leading to the presence of a given small amount of G* at each temperature. According to Table III, the rate of adduct formation, as measured in s^{-1} by dX_2/dt, is indeed many orders of magnitude lower than, for example, the opening rate of the AU base pair as determined from proton exchange (Teitelbaum & Englander, 1975; Mandal et al., 1979). However, another manner to check the consistency of our model is to calculate expected m_D values (relative to denatured DNA) from m_N values (as measured with native DNA) and to compare "calculated" and experimental values of m_D. From (13), one gets $m_D = w m_N$ with

$$w = \frac{K_D}{K_N} \frac{1 + K_N}{1 + K_D} \qquad (23)$$

where K_N and K_D were obtained from the comparison of k_{obsd} and k_3. The values of m and w are given in Table V. Before comparing experimental and calculated values of m_D, the conditions of measurement of k_{obsd} and k_3 relative to those of m have to be explicited. The two first parameters were determined only in 2×10^{-3} M citrate, but m values were obtained from experiments made in 2×10^{-3} M and 10^{-2} M citrate. Actually, we can assume that K is almost independent

Table VI: Comparison of Observed and Calculated Values of Parameter m in Two Possible Cases As Discussed in Section d for AF[a]

	t (°C)				
	4	10	15	20	37
m'_N	0.112	0.166	0.314	0.569	1.05
m'_D (exptl)	0.112	0.185	0.273	0.295	0.295
m'_D (calcd)	(0.64)	(0.82)	(1.47)	2.10	4.63
$(1 + K_N)/(1 + K_D)$	(0.87)	(0.75)	(0.70)	0.65	0.15
$(m'/K)_D$ (exptl)	0.112	0.185	0.273	0.295	0.295
$(m'/K)_D$ (calcd)	0.09	0.12	0.19	0.37	0.16

[a] The first three rows correspond to case i and the last three rows to case ii.

of ionic strength (see Discussion). But, even in the case of a small dependence of K with ionic strength, the range of variation is small enough to be neglected as a first approximation. When, indeed, w values (determined from experiments made in 2×10^{-3} M buffer) are used to calculate m_D from m_N values obtained in 10^{-2} and 2×10^{-3} M buffer the agreement between the experimental and the calculated values of m_D is found reasonably good for both ionic strengths (see Table V).

(d) When a comparison is made between the two carcinogens N-Aco-AAF and N-OH-AF, the reaction scheme was supposed to be different and to depend mainly on the presence of the acetyl group. However, the values of K_N and K_D that measure the G $\rightleftarrows$ G* equilibrium constant in native and denatured DNA, respectively, are essentially independent of the carcinogen. We can therefore calculate m_D values for N-OH-AF, by using the corresponding experimental values of m_N but the K_N and K_D as determined from experiments made with N-Aco-AAF.

In order to check the assumption relative to the mode of binding of N-OH-AF that was made previously, the experimental values of the percentage of modified bases as given in Table II can be interpreted by means of the two types of reaction pathways.

(i) N-OH-AF is supposed to react only with G* in a manner similar to N-Aco-AAF. The parameter ln $(1 - X)/(X - a)$ is thus equal to m' (eq 13) in which the prime refers to AF instead of AAF, since both binding rate constants and solvolysis rate of the two carcinogens must differ. In such a case, the same type of calculation as made with AAF can be applied, leading to calculated values of m_D' from experimental values of m_N'. The comparison between the experimental and calculated values of m_D' given in Table VI indicates clearly that the discrepancies are such as to rule out this type of pathway.

(ii) N-OH-AF is supposed to react only with G ("native" guanine residue). The parameter ln $(1 - X)/(X - a)$ is thus equal to m'/K (see eq 19 and 20), and $(m'/K)_D$ is obviously related to $(m'/K)_N$ by

$$(m'/K)_D = \frac{1 + K_D}{1 + K_N}(m'/K)_N \qquad (24)$$

The values of $(m'/K)_D$ calculated according to (24) are also given in Table VI. The agreement between calculated and experimental values is far better than that in case i and comparable to that obtained with N-Aco-AAF (see Table V).

In addition to this quantitative comparison, it must be pointed out that the plateau value that is observed in Figure 3 for N-OH-AF binding to denatured DNA reflects qualitatively the disappearance of available G conformations according to values displayed in Table V.

Finally, from our data and their interpretations, the following initial assumptions appear to be valid: (a) The electrophilic carcinogens are probes for either G or G*, but the rate of exchange between these two conformations is fast relative to the rate of carcinogen binding. (b) The amount of G*, i.e., of a particular local structure of the nucleotidic chain, is not negligible even at room temperature, and the thermodyamic parameters of the equilibrium, ΔH and ΔS, are 9 kcal mol^{-1} and 27 cal K^{-1} mol^{-1}, respectively. (c) The data obtained in three different series of carcinogen binding studies and with two different carcinogens, the acetylated and the deacetylated forms of aminofluorene, show that these two carcinogens probe two distinct states of the guanine residues in the double helix of DNA: N-OH-AF binds to "native" G residues and N-Aco-AAF to an altered state G* of guanine residues. We now suggest a conformational model for the G $\rightleftarrows$ G* transition that could explain such a specificity.

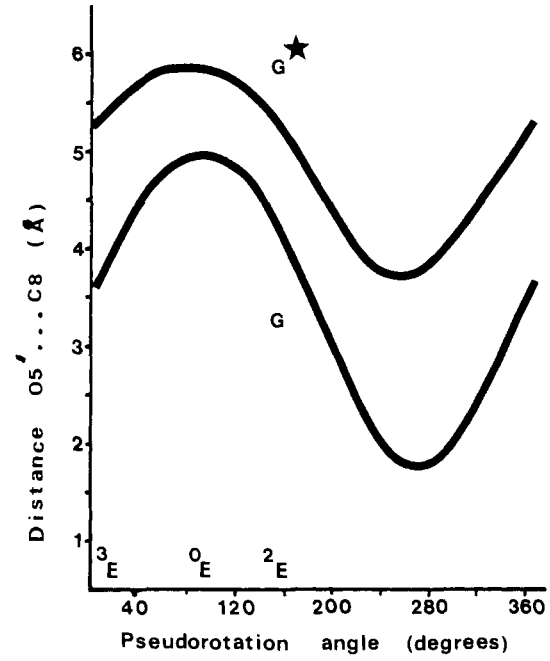

FIGURE 2: Plots of the distance between the C_8 atom of guanine and the O(5') atom of the sugar–phosphate backbone as a function of sugar pucker for two conformations of the torsion angle C(3')–C(4')–C(5'): first, the standard conformation (40°) (gauche$^+$) and then the trans conformation (180°), which is associated with G*. The glycosyl torsion angle, χ, has been left invariant (80°). The pseudorotation angle for the classical C(2')-endo conformation is 162° (B form of DNA), for the classical C(3')-endo conformation it is 18° (A form of DNA), and for the transient O(4')-endo conformation it is 90°. The amount of puckering has been maintained constant.

Discussion

Structural and Dynamic Aspects of Reaction Path. In case of N-OH-AF, the native B conformation of the guanine is required. In such a conformation [C(2')-endo for the sugar, anti for the base, gauche$^+$ for C(4')–C(5'), and double gauche$^-$ for the phosphodiesters], the C_8 of the guanine residues is close to the anionic phosphate. We think this conformation is necessary because the phosphate stabilizes the transient nitrenium ion during the reaction of N-OH-AF with the guanine. But, in the case of N-Aco-AAF, the acetyl group and phosphate group collide, preventing access to the C_8 of the guanine. In Figure 2, the distance between O(5') and C_8 is plotted as a function of the phase angle of pseudorotation. The region denoted by "breathing DNA" covers pseudorotational fluctuations in a broad C(2')-endo region with the accompanied fluctuations in the bases and the sugar–phosphate backbone. In that region, the distance between O(5') and C_8 varies between 2.9 and 4.0 Å. However, even at a distance of 4.0 Å,

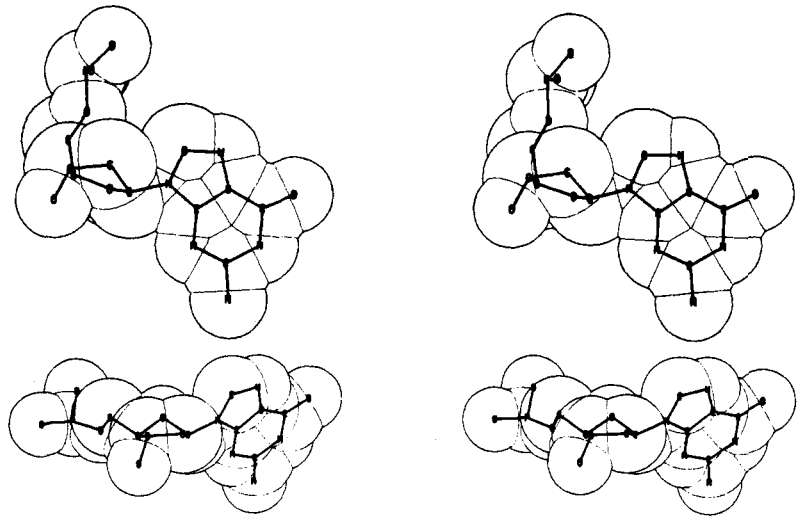

FIGURE 3: A guanine residue in the classical B-form conformation showing the weak accessibility of C_8 (above) and a guanine residue in the proposed G* conformation [O(4′)-endo pucker and trans conformation for C(4′)–C(5′)]. Both views are stereographic drawings of the molecular fragment with van der Waals radii.

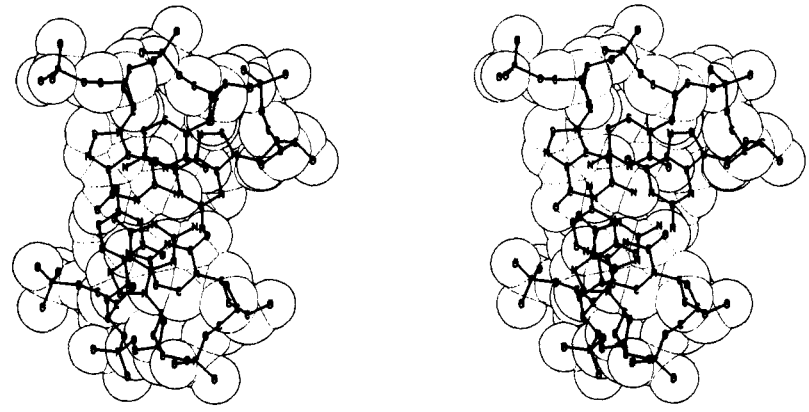

FIGURE 4: Stereographic drawing of the trimer d(G-C)$_3$. On the strand above (G_1-C_2-G_3), the guanine residues are in the "native" conformation and, on the strand below (C_4-G_5-C_6), the guanine residue G_5 is in the proposed G* conformation. The accessibility of C_8 is clearly seen. The model was constructed on an interactive display graphic PS300 from Evans and Sutherland with the program FRODO. The starting coordinates are those from Arnott & Hukins (1972).

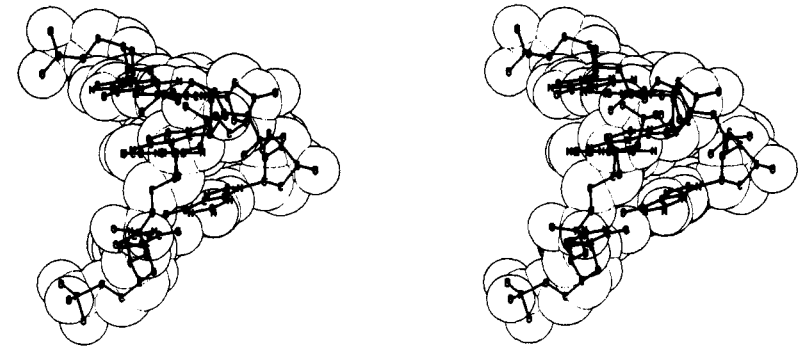

FIGURE 5: Another stereographic drawing of the trimer d(G-C)$_3$ incorporating a G* guanine residue. In this view, the G* residue is on the strand toward the viewer. From those views, it it clear that the distortion of the DNA molecule due to a G* residue is minimal.

the (acetoxyacetyl)amino group of N-Aco-AAF would collide with the phosphate group at O(5′). Therefore, we suggest that the next step is a switch of the torsion angle C(3′)–C(4′)–C(5′)–O(5′) (ψ) from the usual gauche$^+$ (60°) conformation to the trans (180°) conformation. Such a switch is particularly feasible when the sugar reaches the O(4′)-endo pucker in its pseudorotational pathway from C(2′)-endo to C(3′)-endo, since in that conformation the short-range interactions between O(5′) and C_8 stabilizing the gauche$^+$ conformation are ruptured (Sundaralingam, 1974; Yathindra & Sundaralingam, 1974). With the torsion angle ψ in the trans conformation, the distance O(5′)···C_8 is close to 6 Å and the O(5′) is turned away from the C_8 atom toward the outside of the helix (see Figure 3). At the same time, in order to keep the double-stranded helical structure, the phosphodiester torsion angle ω [C(5′)–O(5′)–P–O(3′)] will switch also from its usual gauche$^-$ conformation to the trans conformation (Yathindra & Sundaralingam, 1976; Sundaralingam & Westhof, 1979; Keepers et al., 1982). We identify this double trans conformation for ψ and ω as that conformation, denoted G* above, that the guanine residue should possess to be able to react with the carcinogen (see Figures 4 and 5). The distance P–P is

not substantially changed by this alternative conformation of ψ and ω. However, a transient base-pair opening might occur during the transition from G to G* as well as from G* to G. The fact that the distance between adjacent phosphorus atoms is left largely invariant with respect to the conformational change implies that the conformational part of the free-energy change should not depend on the ionic strength. A difference in guanine reactivity appears however in Table I, when the results obtained in 2×10^{-3} and 10^{-2} M citrate, respectively, are compared. The factor 10 in the amount of AAF bound between the two ionic strengths is due to an overall decrease in reactivity of the carcinogen itself in the presence of DNA, which reveals the role played by the polyelectrolyte properties of the DNA during the approach of a charged species like the nitrenium ion.

Comparison with Hydrogen Exchange Results. It was suggested above that the carcinogen N-Aco-AAF titrates those guanine sites with the torsion angles about C(4′)–C(5′) and P–O(5′) both in the trans domain. At any moment, a certain amount (which depends on the temperature) of such sites exists. The ΔG_0 is between 1.0 and 2.0 kcal/mol and the ΔH_0 around 9.0 kcal/mol with ΔS_0 around 30 cal K^{-1} mol^{-1}. The values are very close to those of Wartell & Benight (1982), 9.424 kcal/mol and 24.8 cal K^{-1} mol^{-1} for ΔH_0 and ΔS_0, respectively. They compare well also with those obtained for hydrogen exchange in poly(rA)·poly(rU) (Preisler et al., 1981), namely, 2.0 kcal/mol for ΔG_0 and for ΔH_0 between 6.7 and 8.2 kcal/mol from infrared and circular dichroism experiments. It has been concluded that hydrogen exchange is a premelting phenomenon occurring far below the melting temperature and involving a single base pair (Kallenbach, 1983; Mirau & Kearns, 1982). It is tempting to suggest that hydrogen exchange and covalent carcinogen binding probe similar torsional changes of the sugar–phosphate of DNA and that both are manifestations of premelting phenomena. However, while carcinogens bind to either the native G structure (N-OH-AF) or the G* altered structure (N-Aco-AAF), hydrogen would exchange in the transiently opened structure occurring during the transition from G to G* or G* to G. Such a mechanism would explain opening kinetics in the 1-s^{-1} range since the opening reaction involves switches between torsional domains and not only torsional *fluctuations* within domains.

Recently, Wilcoxon & Schurr (1983) have shown that the flexural and torsional rigidities of DNA vary only slightly in the temperature range 0–70 °C. Thus, open base pairs do not reduce sufficiently the flexural and torsional rigidities to influence significantly the Brownian dynamics. Such a conclusion is expected in our model of torsional crankshaft motions in the sugar–phosphate backbone as the origin of premelting phenomena, since a torsional switch around one bond is compensated by a torsional switch around another bond in the other direction.

In contrast to the previous methods, our method tests the local dynamics at guanine residues in natural DNA and not in synthetic polymers. Also, it has been shown (Fuchs, 1984) that the distribution of AAF-modified guanines in a fragment of pBR322 is nonuniform, the probability for a guanine to be modified varying between 1 and 40 on a relative scale. This implies that the G $\rightleftarrows$ G* transition depends on the neighboring base pairs. The values given above are, thus, to be understood as averages over the different sites. In other words, over a certain period of time, some guanine residues are more often in the G* state than others. It can be added here that with AF there is no such large variability in the distribution of AF-modified guanines along the same DNA fragment (Bichara & Fuchs, 1985). This is to be expected, since AF probes guanine residues in the "native" conformation.

Dynamics of Adduct. With AAF bound on a guanine, the conformation of the adduct would be close to O(4′)-endo for the sugar, anti for the base, and trans for ψ and ω. Although such a conformation is feasible, it is certainly not the most favorable. The sugar pucker will probably change to another conformation, like C(2′)-endo, C(1′)-exo, C(4′)-exo, or C(3′)-endo. This situation could lead to a destabilization of the double helix and a subsequent conformational rearrangement of the adduct to a conformation where the guanine base is in the syn conformation and on the outside with the fluorene inserted between base pairs in agreement with the insertion–denaturation model (Fuchs & Daune, 1972; Fuchs, 1975; Fuchs et al., 1976; Daune et al., 1981). Alternatively and depending on the base sequence (for example, a stretch of alternating G-C's or more generally Pur-Pyr, it is also conceivable that the conformational rearrangement leads to a local segment of Z-type DNA conformation, with the guanine in the syn orientation but on the inside and the fluorene on the outside (Sage & Leng, 1980; Grunberger & Santella, 1981; Santella et al., 1981b; Hingerty & Broyde, 1982).

On the other hand, N-OH-AF binding to DNA does not induce large conformational alterations. Thus, NMR studies show that AF-modified guanosine preferentially stays in the anti conformation (Leng et al., 1980). Theoretical studies also indicate a preference for the anti domains of the AF-modified guanine (Broyde & Hingerty, 1983). AF-modified DNA is much less sensitive to degradation by S1 endonuclease from *Aspergillus oryzae* (Kriek & Spelt, 1979). Also, specific antibodies studies show that the aminofluorene is partially buried in the interior of the DNA double helix (Spodheim-Maurizot et al., 1979; Sage et al., 1979). The decrease in T_m with an increase in the percentage of modified bases is similar in AF- and AAF-modified DNA (−1.4 °C per percent and −1.15 °C per percent, respectively), but there is no direct relationship between the stability of the double helix, as measured by T_m and any local structural change. Finally, the unwinding of covalently closed circular DNA that was observed after covalent binding of several carcinogens (Drinkwater et al., 1978; Lang et al., 1979) is not induced in the case of AF-modified DNA (unpublished results).

Relationships between the G → G and the B → Z Transitions.* Some time ago, a model was proposed for the B $\rightleftarrows$ Z transition involving correlated crankshaft motions of the sugar–phosphate backbone without breaking of hydrogen bonds (Sundaralingam & Westhof, 1981). Recent NMR (Sarma et al., 1983) and Raman (Wartell et al., 1983) results tend to support such a model for the B $\rightleftarrows$ Z transition. In the model suggested above, the G $\rightleftarrows$ G* transition involves also correlated motions in the sugar–phosphate backbone. Therefore, we suggest that the stereochemical dynamics underlying the G $\rightleftarrows$ G* transition controls also the B $\rightleftarrows$ Z transition in alternating purine–pyrimidine deoxypolymers (Westhof, 1983). The values recently obtained for the energetics of the B $\rightleftarrows$ Z transition (Peck & Wang, 1983) are compatible with such a proposal. If this hypothesis is correct, then those polymers with a high proclivity toward the Z form (Jovin et al., 1983) should be more susceptible to N-Aco-AAF attack. Also, it could be expected that, at the point of the B $\rightleftarrows$ Z transition, guanine residues would be highly susceptible to AAF attack.

Conclusions

Our work brings new data pertaining to the dynamics of the DNA molecule, e.g., a conformational change at the level

of a GC pair. The presence of another local structure, we have called G*, was probed by means of a strong electrophilic reagent, the ultimate carcinogen N-Aco-AAF. Conversely, another electrophilic reagent, N-OH-AF, was used as a probe of the classical B structure. Although the chemical rate of covalent binding of these two molecules to guanine residues was small enough to preclude any dynamical study of the G $\rightleftarrows$ G* equilibrium, values of the equilibrium thermodynamic parameters close to those relative to single base pair opening were found. It is suggested that hydrogen exchange takes place in the transient states occurring during the G $\rightleftarrows$ G* transition.

Other types of physical studies would be necessary to determine precisely the relative amount of G* and the exchange rate between G and G*. In addition to the problem of carcinogen binding or more generally to that of any drug that binds covalently to DNA, this conformational dynamics has to play a role in most of the specific recognition processes between proteins and nucleic acids.

Registry No. N-Aco-AAF, 6098-44-8; N-OH-AF, 53-94-1; deoxyguanosine, 961-07-9.

REFERENCES

Altona, C., & Sundaralingam, M. (1972) *J. Am. Chem. Soc. 94*, 8205.

Arnott, S., & Hukins, D. W. L. (1972) *Biochem. Biophys. Res. Commun. 47*, 1504.

Barkley, M. S., & Zimm, B. H. (1979) *J. Chem. Phys. 70*, 2991.

Bichara, M., & Fuchs, R. P. P. (1985) *J. Mol. Biol.* (in press).

Bolton, P. H., & James, T. L. (1980) *Biochemistry 19*, 1388.

Bresloff, J. L., & Crothers, D. M. (1975) *J. Mol. Biol. 95*, 103.

Broyde, S., & Hingerty, B. (1983) *Biopolymers 22*, 2423.

Crick, F. H. C., & Klug, A. (1975) *Nature (London) 255*, 530.

Daune, M. (1983) in *Structure, Dynamics, Interactions and Evolution of Biological Macromolecules* (Hélène, C., Ed.) pp 57–68, Reidel, Dordrecht, The Netherlands.

Daune, M., Fuchs, R. P. P., & Leng, M. (1981) *Natl. Cancer Inst. Monogr. 58*, 207.

DeBaun, J. R., Miller, E. C., & Miller, J. A. (1979) *Cancer Res. 30*, 577.

De Murcia, G., Lang, M. C., Freund, A. M., Fuchs, R. P. P., Daune, M. P., Sage, E., & Leng, M. (1979) *Proc. Natl. Acad. Sci. U.S.A. 76*, 6076.

Drinkwater, N. R., Miller, J. A., Miller, E. C., & Yang, N. C. (1978) *Cancer Res. 38*, 3247.

Early, T. A., Kearns, D. R., Hillen, W., & Wells, R. D. (1981) *Biochemistry 20*, 3756.

Englander, S. W., Kallenbach, N. R., Heeger, A. J., Krumhansl, J. A., & Litwin, S. (1980) *Proc. Natl. Acad. Sci. U.S.A. 77*, 7222.

Fuchs, R. P. P. (1975) *Nature (London) 257*, 151.

Fuchs, R. P. P. (1984) *J. Mol. Biol. 177*, 173–180.

Fuchs, R. P., & Daune, M. (1972) *Biochemistry 11*, 2659.

Fuchs, R. P. P., Lefèvre, J. F., Pouyet, J., & Daune, M. (1976) *Biochemistry 15*, 3347.

Fuchs, R. P. P., Lang, M. C. E., Miller, E. C., & Miller, J. A. (1981) *Carcinogenesis 2*, 655.

Genest, D., & Wahl, P. (1978) *Biophys. Chem. 7*, 317.

Grunberger, D., & Santella, R. M. (1981) *J. Supramol. Struct. 17*, 231.

Hingerty, B., & Broyde, S. (1982) *Biochemistry 21*, 3243.

Hogan, M. E., & Jardetzky, O. (1979) *Proc. Natl. Acad. Sci. U.S.A. 76*, 6341.

Hurley, I., Osei-Gyimah, P., Archer, S., Scholes, C. P., & Lerman, L. S. (1982) *Biochemistry 21*, 4999.

Jovin, T. M., McIntosh, L. P., Arndt-Jovin, D. J., Zarling, D. A., Robert-Nicoud, M., van de Sande, J. H., Jorgenson, K. F., & Eckstein, F. (1983) *J. Biomol. Struct. Dyn. 1*, 21.

Kallenbach, N. R. (1983) in *Structure, Dynamics, Interactions and Evolution of Biological Macromolecules* (Hélène, C., Ed.) p 69, Reidel, Dordrecht, The Netherlands.

Kapuler, A. M., & Michelson, A. M. (1971) *Biochim. Biophys. Acta 232*, 436.

Keepers, J. W., Kollman, P. A., Weiner, P. K., & James, T. L. (1982) *Proc. Natl. Acad. Sci. U.S.A. 79*, 5537.

Kilpatrick, J. E., Pitzer, K. S., & Spitzer, R. (1947) *J. Am. Chem. Soc. 64*, 2483.

Kollman, P. A., Keepers, J. W., & Weiner, P. K. (1982) *Biopolymers 21*, 2345.

Kriek, E., & Spelt, C. E. (1979) *Cancer Lett. (Shannon, Irel.) 7*, 147.

Lang, M. C. E., Freund, A. M., de Murcia, G., Fuchs, R. P. P., & Daune, M. P. (1979) *Chem.-Biol. Interact. 28*, 171.

Leng, M., Ptak, M., & Rio, P. (1980) *Biochem. Biophys. Res. Commun. 96*, 1095.

Mandal, C., Kallenbach, N. R., & Englander, S. W. (1979) *J. Mol. Biol. 135*, 391.

McConnell, B., & Von Hippel, P. H. (1970) *J. Mol. Biol. 50*, 297.

Miller, J. A. (1970) *Cancer Res. 30*, 559.

Mirau, P. A., & Kearns, D. R. (1983) in *Structure and Dynamics: Nucleic Acids and Proteins* (Clementi, E., & Sarma, R. H., Eds.) p 227, Adenine Press, New York.

Olson, W. K. (1981) in *Biomolecular Stereodynamics* (Sarma, R. H., Ed.) p 327, Adenine Press, New York.

Palecek, E. (1976) *Prog. Nucleic Acid Res. Mol. Biol. 18*, 151.

Peck, L. J., & Wang, J. C. (1983) *Proc. Natl. Acad. Sci. U.S.A. 80*, 6206.

Preisler, R. S., Mandal, C., Englander, S. W., Kallenbach, N. R., Howard, F. B., Frazier, J., & Miles, H. T. (1981) in *Biomolecular Stereodynamics* (Sarma, R. H., Ed.) p 405, Adenine Press, New York.

Printz, M. P., & Von Hippel, P. H. (1968) *Biochemistry 7*, 3194.

Ramstein, J., & Leng, M. (1975) *Biophys. Chem. 3*, 234.

Rio, P., & Leng, M. (1983) *Nucleic Acids Res. 11*, 4947.

Sage, E., & Leng, M. (1980) *Proc. Natl. Acad. Sci. U.S.A. 77*, 4597.

Sage, E., Fuchs, R. P. P., & Leng, M. (1979) *Biochemistry 18*, 1328.

Santella, R. M., Grunberger, D., Weinstein, I. B., & Rich, A. (1981a) *Proc. Natl. Acad. Sci. U.S.A. 78*, 1451.

Santella, R. M., Grunberger, D., Broyde, S., & Hingerty, B. E. (1981b) *Nucleic Acids Res. 9*, 5459.

Sarma, M. H., Gupta, G., Dhingra, M. M., & Sarma, R. H. (1983) *J. Biomol. Struct. Dyn. 1*, 59.

Simon, E. M. (1971) *J. Chem. Phys. 54*, 4738.

Sobell, H. M., Reddy, B. S., Bhandary, K. K., Jain, S. C., Sakore, T. D., & Seshadri, T. P. (1977) *Cold Spring Harbor Symp. Quant. Biol. 42*, 87.

Spodheim-Maurizot, M., Saint-Ruf, G., & Leng, M. (1979) *Nucleic Acids Res. 6*, 1683.

Sturm, J., Zana, R., & Daune, M. (1975) *Biochim. Biophys. Acta 407*, 43.

Sundaralingam, M. (1974) *Int. J. Quantum Chem., Quantum Biol. Symp. No. 1*, 81.

Sundaralingam, M., & Westhof, E. (1979) *Int. J. Quantum Chem., Quantum Biol. Symp. No. 6*, 115.

Sundaralingam, M., & Westhof, E. (1980) *Biophys. J. 32*, 250.
Sundaralingam, M., & Westhof, E. (1981) in *Biomolecular Stereodynamics* (Sarma, R. H., Ed.) p 301, Adenine Press, New York.
Swicord, M. L., & Davis, C. C. (1982) *Biopolymers 21*, 2453.
Teitelbaum, H., & Englander, S. W. (1975) *J. Mol. Biol. 92*, 55.
Urabe, H., & Tominaga, Y. (1982) *Biopolymers 21*, 2477.
Van Zandt, L. L., Kohli, M., & Prohofsky, E. W. (1982) *Biopolymers 21*, 1465.
Wahl, P., Paoletti, C., & Le Pecq, J. B. (1970) *Proc. Natl. Acad. Sci. U.S.A. 65*, 417.
Wartell, R. M., & Benight, A. S. (1982) *Biopolymers 21*, 2069.
Wartell, R. M., Harrell, J. T., Zacharias, W., & Wells, R. D. (1983) *J. Biomol. Struct. Dyn. 1*, 83.
Westhof, E. (1983) *NATO-CECAM Workshop*, Orsay, France, University of Orsay, Paris.
Wilcoxon, J., & Schurr, J. M. (1983) *Biopolymers 22*, 2273.
Woodward, C. K., & Hilton, B. D. (1979) *Annu. Rev. Biophys. Bioeng. 8*, 99.
Yathindra, N., & Sundaralingam, M. (1974) *Biopolymers 13*, 2061.
Yathindra, N., & Sundaralingam, M. (1976) *Nucleic Acids Res. 3*, 729.

Alternative Conformers of 5S Ribosomal RNA and Their Biological Relevance†

Anni Christensen,‡ Merete Mathiesen,‡ Debra Peattie,§,‖ and Roger A. Garrett*,‡

Division of Biostructural Chemistry, Kemisk Institut, Aarhus Universitet, DK-8000 Aarhus C, Denmark, and Department of Biochemistry and Molecular Biology, The Biological Laboratories, Harvard University, Cambridge, Massachusetts 02138

Received July 26, 1984

ABSTRACT: Different conformational states of *Escherichia coli* 5S ribosomal RNA that may participate in protein biosynthesis have been either detected experimentally or predicted on the basis of phylogenetic sequence comparisons. The A conformer exists in a high-salt form (A_H) that binds ribosomal proteins and assembles into the 50S subunit and in a low-salt form (A_L), of uncertain biological relevance, that binds at least one ribosomal protein and differs in tertiary structure from the A_H form. Experimentally, the A_H form has been investigated comprehensively and the A_L form partially. There is also a B conformer that exhibits an altered secondary structure and does not assemble with ribosomal proteins. For this conformer to be functionally active, it must be both discrete and universal among 5S RNAs. Here, we examine its structure by employing single and double strand specific ribonucleases and nucleotide-specific chemical reagents. We demonstrate that the B form exhibits a secondary structure only a part of which is both universal and conformationally homogeneous, and we conclude, therefore, that the whole B form cannot participate in protein biosynthesis. We note, however, that progressive structural changes occur during the transitions $A_H \rightarrow A_L \rightarrow B$ and provide evidence that the structural alteration during the transition $A_H \rightarrow A_L$ may be universal, which reinforces the view that the A_L form is of biological relevance.

One of the most important and unresolved questions concerning RNA function is can RNA operate by the interconversion of alternative conformers? A very specific mechanism was suggested for the interaction and relative movement of tRNA and mRNA by Woese (1970), and more general proposals have been made for reversible and putative 5S RNA–tRNA interactions (Fox & Woese, 1975; Weidner et al., 1977). More recently, comparative sequence studies on the large ribosomal RNAs have also revealed alternative and conserved base-pairing schemes, exhibiting approximately similar free energies [reviewed by Noller (1980) and Brimacombe et al. (1983)].

The 5S ribosomal RNA is small; it interacts with a group of proteins and lies in a functionally important region of the 50S subunit. For these reasons, it has been chosen for many seminal studies on RNA structure, RNA–protein interactions, and RNA function [reviewed by Garrett et al. (1981)]. Some of the studies on the RNA structure that employed biochemical and spectroscopic techniques have yielded evidence for major and minor conformational changes occurring in 5S RNA under solution conditions close to physiological, at least some of which were induced by ribosomal proteins [reviewed by Monier (1974) and Garrett et al. (1981)]. The best characterized transition is between the native A and B conformers (A and B forms) of the *Escherichia coli* 5S RNA (Aubert et al., 1968) that occurs in the absence of ribosomal proteins. It requires an activation energy of 65 kcal/mol and involves the disruption and re-forming of an estimated nine base pairs (Richards et al., 1973). A less dramatic change has also been recorded within the tertiary structure of the A form (A_H to A_L) that is salt dependent and occurs close to physiological pH and over a time scale compatible with the translation process (Kao & Crothers, 1980; Kime & Moore, 1982; Rabin et al., 1983).

The native A form has been subjected to both sequence comparison studies and experimental probing, and there is now

† The research was supported by grants from the Danish Science Research Council, the Carlsberg Foundation, and the Aarhus University Fund.
‡ Division of Biostructural Chemistry, Aarhus Universitet.
§ Department of Biochemistry and Molecular Biology, Harvard University.
‖ Present address: Department of Biochemistry, Stanford University, School of Medicine, Stanford, CA 94305.

0006-2960/85/0424-2284$01.50/0